Naval Research Laboratory

Washington, DC 20375-5320

NRL/MR/7634--20-10,168

Coordinated Ionospheric Reconstruction Cubesat Experiment (CIRCE) Sun Sensor Testing Results

S. A. Budzien

C. M. Brown

A. W. Stephan

A. C. Nicholas,

K. F. Dymond

T. T. Finne

Geospace Science and Technology Branch
Space Science Division

B. A. Fritz

NRC Postdoctoral Research Associate
Space Science Division

K. D. Wolfram

Technology Service Corporation
Arlington, VA

January 29, 2021

REPORT DOCUMENTATION PAGE

Form Approved
OMB No. 0704-0188

1. REPORT DATE *(DD-MM-YYYY)*	**2. REPORT TYPE**	**3. DATES COVERED** *(From - To)*
29-01-2021	NRL Memorandum Report	Dec 15 2019 – Dec 31 2019

4. TITLE AND SUBTITLE

Coordinated Ionospheric Reconstruction Cubesat Experiment (CIRCE) Sun Sensor Testing Results

5a. CONTRACT NUMBER

5b. GRANT NUMBER

5c. PROGRAM ELEMENT NUMBER
62435N

6. AUTHOR(S)

S. A. Budzien, C. M. Brown, A. W. Stephan, B. A. Fritz*, A. C. Nicholas, K. F. Dymond, K. D. Wolfram**, and T. T. Finne

5d. PROJECT NUMBER

5e. TASK NUMBER

5f. WORK UNIT NUMBER
1F44

7. PERFORMING ORGANIZATION NAME(S) AND ADDRESS(ES)

Naval Research Laboratory
4555 Overlook Avenue, SW
Washington, DC 20375-5320

8. PERFORMING ORGANIZATION REPORT NUMBER

NRL/MR/7634--20-10,168

9. SPONSORING / MONITORING AGENCY NAME(S) AND ADDRESS(ES)

Office of Naval Research
One Liberty Center
875 N. Randolph Street, Suite 1425
Arlington, VA 22203-1995

10. SPONSOR / MONITOR'S ACRONYM(S)
ONR

11. SPONSOR / MONITOR'S REPORT NUMBER(S)

12. DISTRIBUTION / AVAILABILITY STATEMENT

DISTRIBUTION STATEMENT A: Approved for public release; distribution is unlimited.

13. SUPPLEMENTARY NOTES

*NRC Postdoctoral Research Associate, 4555 Overlook Ave., S.W., Washington, DC 20375-5320
**Technology Service Corporation, 25118th St South, Suite 705, Arlington, VA 22202

14. ABSTRACT

A new class of compact, high-sensitivity three-channel photometers has been developed by NRL for ionospheric remote sensing from CubeSats and other platforms. The photometer can only be used when the Sun is out of the field-of-view and is protected by a sun sensor. This report reviews the compact sun sensor design, characterizes its field-of-view, measures its response to solar illumination, and suggests future improvements.

15. SUBJECT TERMS

Photometer Remote sensing Airglow Ionosphere
Nightglow Aeronomy Methods

16. SECURITY CLASSIFICATION OF:			**17. LIMITATION OF ABSTRACT**	**18. NUMBER OF PAGES**	**19a. NAME OF RESPONSIBLE PERSON**
a. REPORT	**b. ABSTRACT**	**c. THIS PAGE**			Scott Budzien
Unclassified Unlimited	Unclassified Unlimited	Unclassified Unlimited	Unclassified Unlimited	18	**19b. TELEPHONE NUMBER** *(include area code)* (202) 767-9372

This page intentionally left blank.

CONTENTS

FIGURES

TABLES

EXECUTIVE SUMMARY

The Coordinated Ionospheric Reconstruction CubeSat Experiment (CIRCE) is a mission that will investigate space weather phenomena in the ionosphere-thermosphere system using a suite of remote sensing and *in situ* instruments. The high-sensitivity, compact Triple Tiny Ionospheric Photometers (Tri-TIPs) were developed at NRL for observing the far-ultraviolet (FUV) 135.6 nm emission of atomic oxygen naturally produced by the nighttime ionosphere. Two Tri-TIPS will be deployed on each satellite viewing different directions to perform tomographic reconstructions of the ionosphere. Since these sensors can only operate at night and when the sun angle is sufficiently outside the field-of-view, each sensor was outfitted with a sun sensor for sensor protection. The sun sensor was custom-designed and built for Tri-TIP. We present characterization of the sun sensor angular field of view in-track and cross track and measurements of the sensitivity threshold. Since this sun sensor design will also be used on follow-on missions and can be adapted to other instruments, we present recommendations for improvements in future applications.

This page intentionally left blank.

COORDINATED IONOSPHERIC RECONSTRUCTION CUBESAT EXPERIMENT (CIRCE) SUN SENSOR TESTING RESULTS

1. INTRODUCTION

1.1 The CIRCE Experiment Concept

The Coordinated Ionospheric Reconstruction CubeSat Experiment (CIRCE) is a joint US-UK mission that will investigate space weather phenomena in the ionosphere-thermosphere system using a suite of remote sensing and *in situ* instruments [Nicholas et al., 2019]. CIRCE will provide multi-point measurements from two 6U CubeSats flying in lead-trail formation in a single orbital plane (Fig. 1). For this mission NRL has contributed two 1U Triple Tiny Ionospheric Photometers (Tri-TIPs) per satellite for observing the far-ultraviolet (FUV) 135.6 nm emission of atomic oxygen naturally produced by the nighttime ionosphere. The primary Tri-TIP objective is to specify the vertical and horizontal distribution of electrons in the ionosphere and characterize the variations of the Equatorial Ionization Anomaly (EIA) [Dymond et al., 2017]. The methodology used to reconstruct the nighttime ionosphere employs continuous UV photometry from five distinct viewing angles in combination with an additional data source (such as *in situ* plasma density measurements) with advanced image space reconstruction algorithm tomography techniques [Dymond et al., 2017]. CIRCE observations will enable further understanding of the driving processes of ionospheric phenomena distributed over latitude and altitude by tying together ion/neutral composition with vertical structure in electron density over a wide range of latitudes.

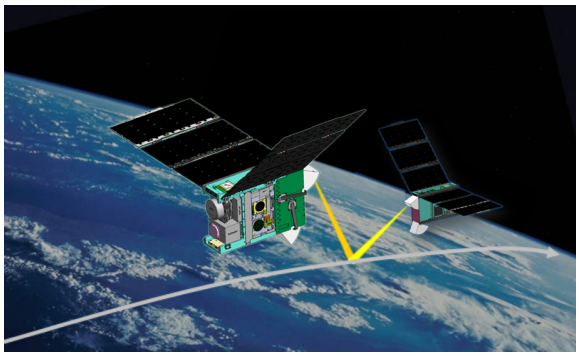

Figure 1. Artist's conception of the dual CubeSat CIRCE mission for characterizing the nighttime ionosphere.

1.2 Triple Tiny Ionospheric Photometer (Tri-TIP)

The Tri-TIP instrument is an ultra-compact three-channel photometer designed to fit within a 10 cm x 10 cm x 10 cm (1U) volume to maximize accommodation opportunities on CubeSats and other platforms. To achieve high sensitivity and multiple channels in this compact form factor, this FUV photometer utilizes: (1) the spectral simplicity of the nighttime ionospheric airglow; (2) a heated long-pass filter; (3) a far-ultraviolet/visible beam splitter separator; and (3) one high voltage power supply to drive three cesium iodide (CsI) photomultiplier tubes (PMTs). These innovations eliminate dispersive optics and enable monitoring multiple channels simultaneously. The algorithm for deriving airglow signals from the three-channel photometers is described elsewhere [Budzien et al., 2018].

The optical layout and operation of the sensor is straightforward (Fig. 2). The hinged deployable mirror assembly in its stowed configuration acts as a dust cover to keep dust and debris from entering the instrument during storage, testing, shipping, and launch. Once deployed, this pick-off mirror directs light from the Earth's atmosphere into the instrument, through a two-vane baffle, to an off-axis parabola

Manuscript approved January 27, 2021.

focusing mirror. Both mirrors are treated with a magnesium fluoride (MgF_2) over aluminum (Al) reflective coating optimized for the far-ultraviolet. The light passes a shutter and solenoid assembly designed to protect the photomultiplier tubes (PMTs) from being exposed to direct sunlight. The shutter solenoid is actuated by a sun-sensor in the electronics stack that is oriented towards the deployed mirror. After going through the open shutter, light passes through a strontium fluoride (SrF_2) long-pass filter. The remaining, converging light is divided by a beam splitter between two PMTs at the prime focus, directing the half of the light towards the UV PMT from the front surface, and the other half through the beam splitter filter towards the red leak PMT. The three Tri-TIP detectors are Hamamatsu R13194 PMTs driven at 1000 V, to monitor the UV signal, the red leak signal and the dark background (including South Atlantic Anomaly and other high energy radiation). The fields-of-view at the PMT are 3° x 6° for the 45° and nadir versions and 0.2° x 6° for the limb version. The far-ultraviolet sensitivity of the sensors is high, roughly 200 counts/sec/Rayleigh for the larger field-of-view, and 14 counts/sec/Rayleigh for the limb view.

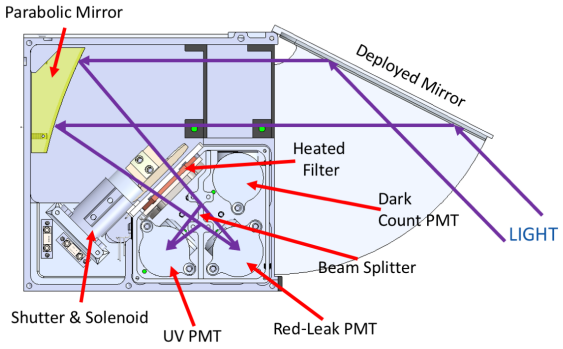

Figure 2. This schematic shows a cutaway version of Tri-TIP with the light path and major optical components labelled.

1.3 The Tri-TIP Sun Sensor

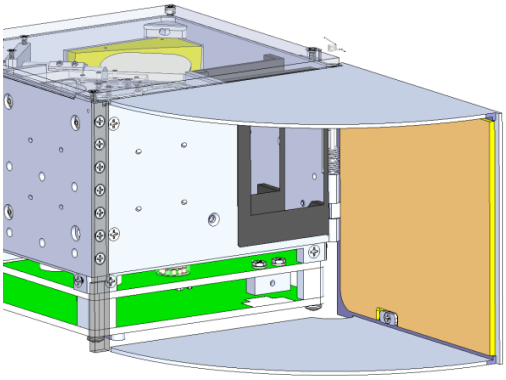

Figure 3. The sun sensor housing is mounted on the sensor electronics card and views the pickoff mirror of most instruments. A sidewall (not shown) with a 3 mm dia. aperture covers most of the sun sensor.

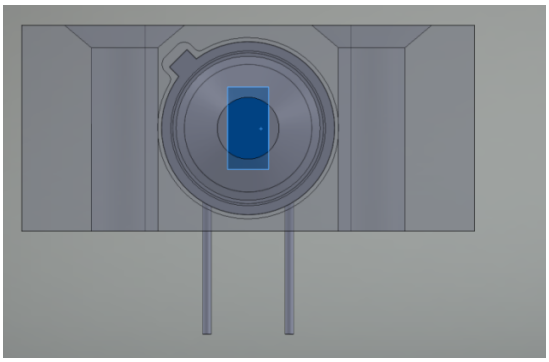

Figure 4. The asymmetrical active area and mount orientation yields slightly different cross-track and in-track fields-of-view, though a significant portion of the larger cross-track field-of-view may be obscured.

The Tri-TIP sun sensor is a custom-designed miniature electrical-optical sensor and associated support circuitry which is integrated into each Tri-TIP instrument. The diode is permanently located on the sensor electronics card, mounted in a housing, and continuously peers through a porthole in the wall to the pick-off mirror, in most cases (Fig. 3). The Sun may be viewed directly in the case of the nadir photometer with the pickoff mirror swung out of the way. The nominal field-of-view results from an asymmetrical active area behind the circular aperture (Fig. 4). The intrinsic field-of-view is therefore 41° cross-track and 30° in-track, but due to asymmetrical placement of the sun sensor with respect to the two dog-ear sun shades, nearly half of the cross-track field-of-view is obscured.

The design is based upon an OSI Optoelectronics PIN-3CDPI diode. The circuit feeds the A/D converter incorporated into the Instrument Data Controller (IDC) electronics card (Fig. 5). The sun

sensor is monitored at 10 Hz and filtered in the Tri-TIP's IDC FPGA for 400 msec, meaning the reading must be above threshold for 4 samples before the "sun sensor over threshold" signal will be triggered. This signal is used by the firmware to automatically switch the sensor temporarily to a safe configuration with high voltage switched off and the shutter closed. The sun sensor threshold itself is adjustable by command; the default value from the software ICD is 0x0126 (equivalent to an analog value of 0.24 V). Moreover, the duration of the temporary safe mode can be set by a command; the default value is 0x012C or 300 seconds.

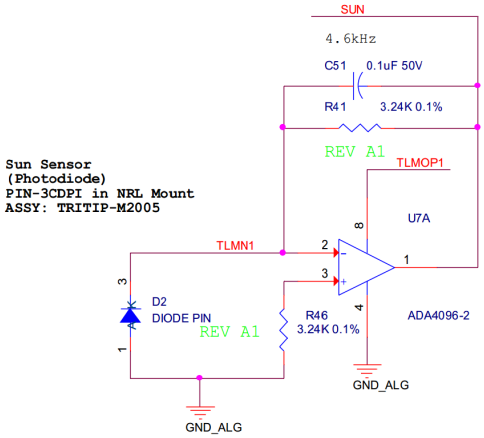

Figure 5. The sun sensor circuit output feeds the Tri-TIP A/D converter and is monitored by the FPGA.

Initial testing of the photodiode was performed at Silver Electronics, Inc. using the sun sensor in its housing. These results are consistent with a roughly 45° FWHM field-of-view for the sun sensor. These preliminary tests measured the photodiode current itself, whereas subsequent tests described in this document record A/D converted voltages reported by the engineering unit FPGA circuitry.

Table 1. Initial Sun Sensor Tests

Direction/Comment	Photodiode (µA)
Office Ambient	0.6
Moon (Direct)	0.6
Horizon 0°	80.2
15°	127
30°	205
45°	330
60°	450
75°	625
Sun 90°	1162

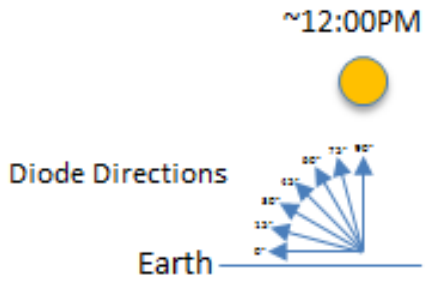

Figure 6. Photodiode orientations during the initial signal level test.

2. TRI-TIP SUN SENSOR TESTS

Objective: To evaluate the relative sensitivity and angular field-of-view of the assembled Tri-TIP sun sensor in an Engineering Model (EM) unit, and measure thresholds for CIRCE/Tri-TIP sun sensors.

- The test verifies the approximate response of the Sun sensor to a bright, collimated visible light source; measures the vertical (in-track) and horizontal (cross-track) angular fields-of-view; and estimates the sun sensor threshold using the Sun outdoors.
- The test was conducted on an optical table located in Bldg. 209, Rm 122A laboratory and on the roof of Bldg. 209.

Payoff: This test will verify sun sensor performance and define threshold values for CIRCE mission operations. Moreover, improvements recommended here can be incorporated into future versions of these sensors that will fly on other, future missions.

2.1 Indoor Test Set-up and Procedure

2.1.1 Equipment required:

- ESD statics pad, wrist strap, and cart
- Tri-TIP EM unit, a black Kapton EM aperture mask, EM test adapter board, HV red warning light, electrical harnesses, and laptop computer
- Test adapter EGSE software
- Dual low voltage power supply (+/-/GND)
- Four multimeters to monitor voltages and currents
- ORIEL Sun Lamp and ORIEL constant current power supply
- Optical table, optical mounts, iris, collimating lens, autocollimation flat mirror
- Alt-Az telescope mount with angular read-outs and continuously adjustable angles
- 3-D printed EM holder and mounting screws

Figure 7: (Left) The benchtop test setup, including sun lamp, iris, collimating lens, and telescope mount to hold the sensor. (Right) Electrical and computer configuration for Tri-TIP power and data collection.

2.1.2 Optical Set-up and Test Procedure

Before the sun sensor test can begin, a collimated light source must be set up with adequate beam size to illuminate the EM sensor on the tripod.

1. Connect the ORIEL lamp (N041236) to the ORIEL 68830 Constant Current Power Supply (N041650) and turn on the lamp to half-power (180.0W). (Items are on loan from Sam Tun, Code 7684). According to Sam Tun, the lamp is approximately 1/3 the brightness of the sun when at full power (360W).
2. Focus the lamp filament on the iris opening with the built-in lamp lens. Orient the lamp aperture, the iris (narrowed to its minimum), and the collimating lens (4" diameter, Aero-Ektar f/6, 24" focal length) on a common optical axis. Make sure the light exiting the iris fills the 4.5" diameter of the Aero-Ektar. Place and adjust the Aero-Ektar one focal length (24") from the iris (with its focus at the real image of the lamp filament).

3. Adjust focus to achieve an approximately collimated beam parallel to the table.
4. Place the printed EM adapter atop the alt-az telescope mount, and adjust the mount to be in the collimated beam. Make sure that the sun sensor will be near the beam center. Place a flat mirror in the holder placing the rear surface of the mirror against the reference surface of the mount. Stop-down the iris to 2 mm. Autocollimate the reflected beam back to an in-focus image of the iris centered on itself, adjusting the focus and telescope mount to establish the beam normal (Fig. 8). Record the angular telescope mount scale readings when normal to the beam.

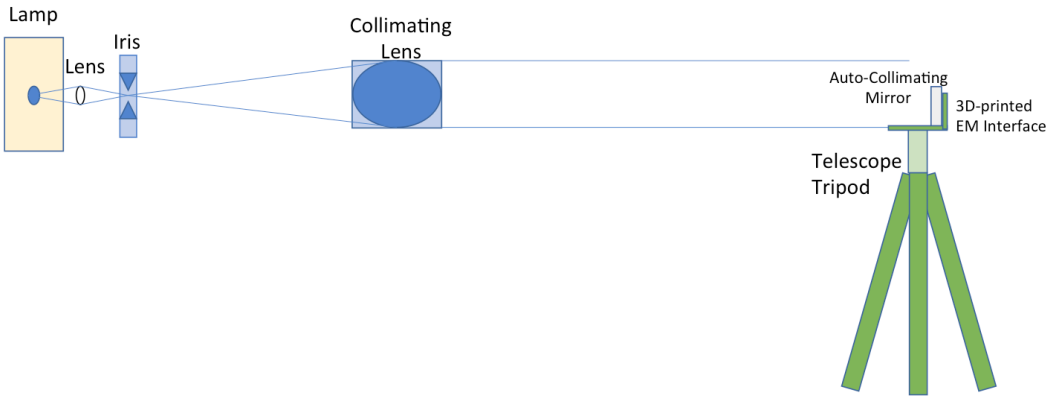

Figure 8: Schematic for setting up the sun lamp to perform autocollimation.

5. Make sure the EM aperture is covered by the opaque, black Kapton tape cover. Open up the iris aperture to 30 mm, then replace the mirror with the NADIR configuration of the EM unit (Fig. 9) and tighten the mounting screws. Record the sun sensor brightness in the normal location. Perform the measurement of sun sensor signal with respect to in-track angle of the EM unit.
6. Repeat, but with the 45F/45R configuration for in-track angle. (The pickoff mirror needs to be repositioned, and the mount may need to repositioned in the beam.)
7. Repeat, but with the LIMB configuration for in-track angle. (The pickoff mirror needs to be repositioned again, and the mount may need to repositioned in the beam.)
8. Repeat, but with the cross-track LIMB configuration cross-track. This should be similar for all orientations due to the dog-ear blockages. Ensure that for the range of motion the EM unit remains in the beam.

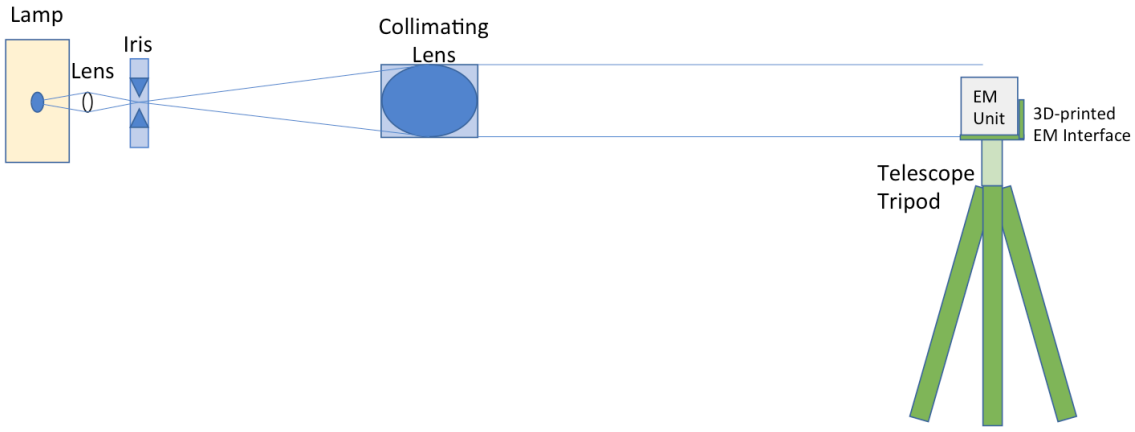

Figure 9: Schematic for measuring Tri-TIP sun sensor angular field-of-view.

2.2 NADIR configuration, vertical direction 2019/12/16

This is a coarse initial angular scan, but provides dark and ambient response, too. This revealed the reflections and shadows near the sun sensor and defined the angular resolution for subsequent scans.

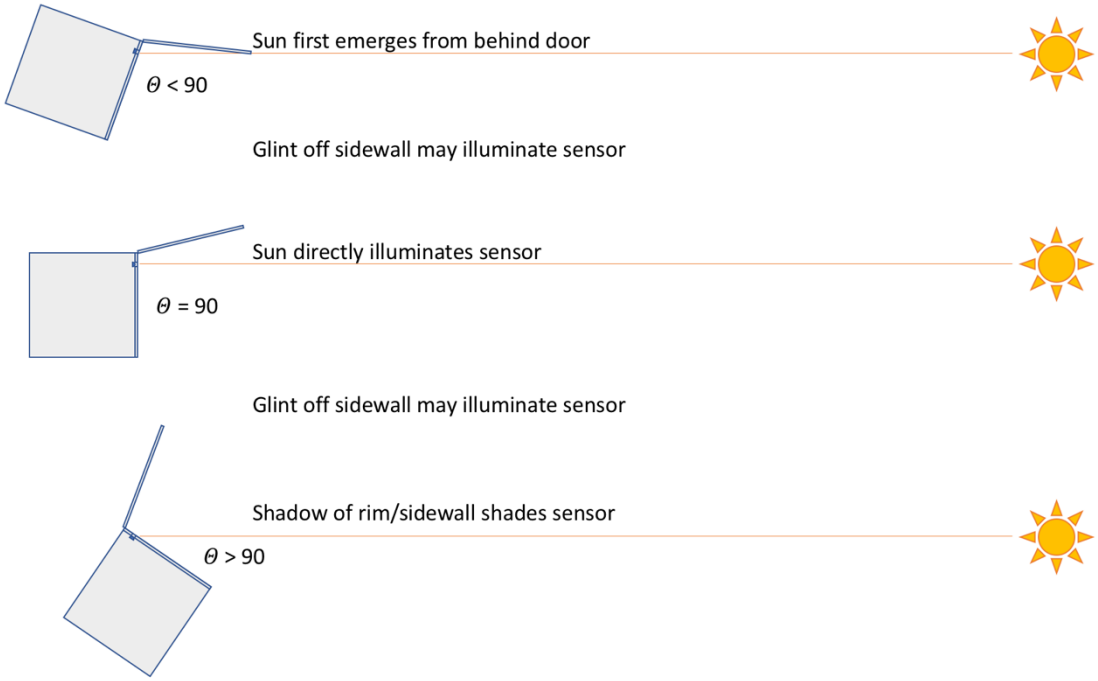

Figure 10: Scanning the nadir sensor vertically shows some configurations that will be encountered. Several minor glints were noted when the light struck the edges of the aperture in the sidewall covering the sun sensor.

The following table shows the initial, coarse readings for the test board interface software reflecting the Sun Sensor Analog and the raw hexadecimal read-out for the Sun Sensor. The peak brightness was roughly 0.28 V for normal incidence. Note that the telescope mount scale measures degrees, but that the tick marks were 2° and that the tripod mount had a maximum angle of 90°, after which degrees started counting down to zero again. The angles reported here are the user-converted angles, not the direct telescope mount readings. Comments about shadows and reflections refer to Figure 10.

Table 2. Test 1: Nadir, vertical

Angle (deg)	Sun (V)	Sun (hex)	Comment
n/a	0.004	005	Tri-TIP door closed
87.5	0.004	005	Beam blocked, ambient room light at sensor
87.5	0.277	156	Normal to beam
100	0.111	08A	12.5 deg past beam
110	0.010	00C	
120	0.037	02E	
87.5	0.281	158	
80	0.120	095	7.5 deg the other side of the beam
70	0.015	00B	
60	0.023	010	
50	0.076	05E	
40	0.024	01D	

2.3 NADIR configuration, vertical direction 2019/12/18

This presents a finer angular scan than the initial measurements.

Table 3. Test 2: Nadir, vertical

Angle (deg)	Sun (V)	Sun (hex)	Comment
87.5	0.269	14E	Normal to beam
94	0.189	0EA	
98	0.107	085	
104	0.030	025	
108	0.010	00D	
114	0.015	012	
120	0.029	024	Sidewall rim shadow crossing sensor
125	0.035	02A	
130	0.015	012	Door shadow covers sensor
135	0.004	005	
140	0.013	01D	
118	0.027	020	
115	0.015	013	Sidewall rim shadow
100	0.049	03D	

Angle (deg)	Sun (V)	Sun (hex)	Comment
90	0.242	12C	
85	0.268	14D	
80	0.210	105	
75	0.099	07B	
70	0.020	019	
65	0.013	010	
60	0.017	015	
55	0.039	030	
50	0.073	05A	
45	0.064	050	
40	0.027	021	Sidewall rim shadow at sensor
35	0.011	00E	
30	0.006	007	Sidewall rim shadow crosses sensor
87.5	0.274	154	

The two data sets for the NADIR configuration taken for both days are plotted together in Figure 11. The largest source of angular error was due to parallax by the observer, since the angular ticks were displaced from the angle indicator. This error may be up to ±2° and can be expected to vary non-randomly from observer to observer; the random error in angle was on the order of ±0.5°. The error in sun signal voltage reading was quite low and varied only ±1 mV.

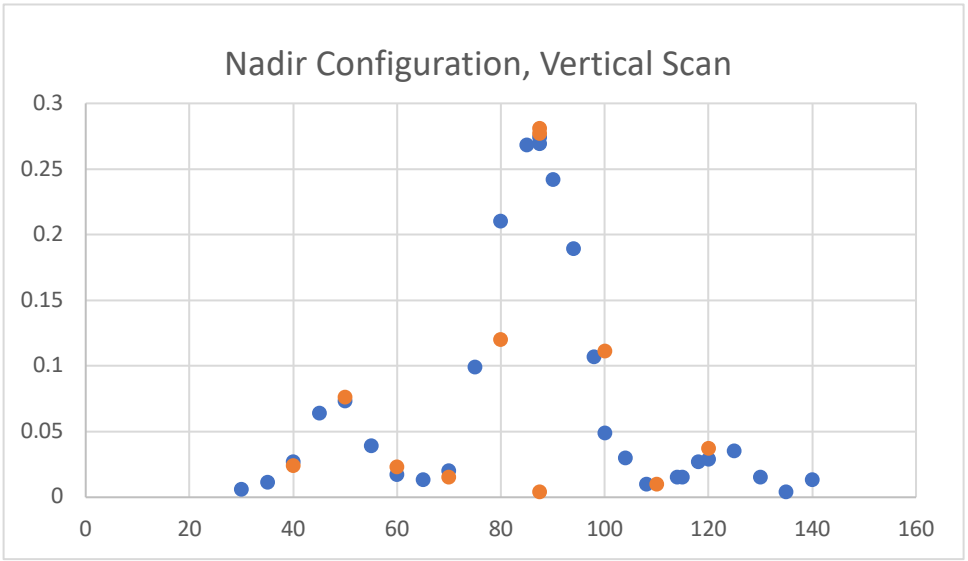

Figure 11. The vertical scans of the sun sensor response for the nadir configuration (with the door fully open). The main response is an 18° FWHM sun sensor response for direct stimulation, while the smaller responses correspond to glints from the edges of the aperture through which the sensor views. The low value (red) at the central peak reflects the response of the sensor to ambient laboratory light. The raw response shown is not normalized, showing good lamp stability day-to-day; a small angle reading error may be present in the red dots from the coarse angle scale.

2.4 45R/45F Configuration, vertical direction 2019/12/18

In this configuration the pickoff mirror for the EM unit was set to a 67.5° opening, corresponding to a 45° reflection, and taped in place. The incidence of direct sun, reflection, and shadow was somewhat different in this configuration (Figure 12) than for the nadir case, due to reflections from the pickoff mirror. Additionally, the smaller door opening reduced the signatures of secondary glints at ±40° from the main response, which are attributed to reflections from the aperture walls (Figure 13): the narrower acceptance angle cut off those wider-angle reflections.

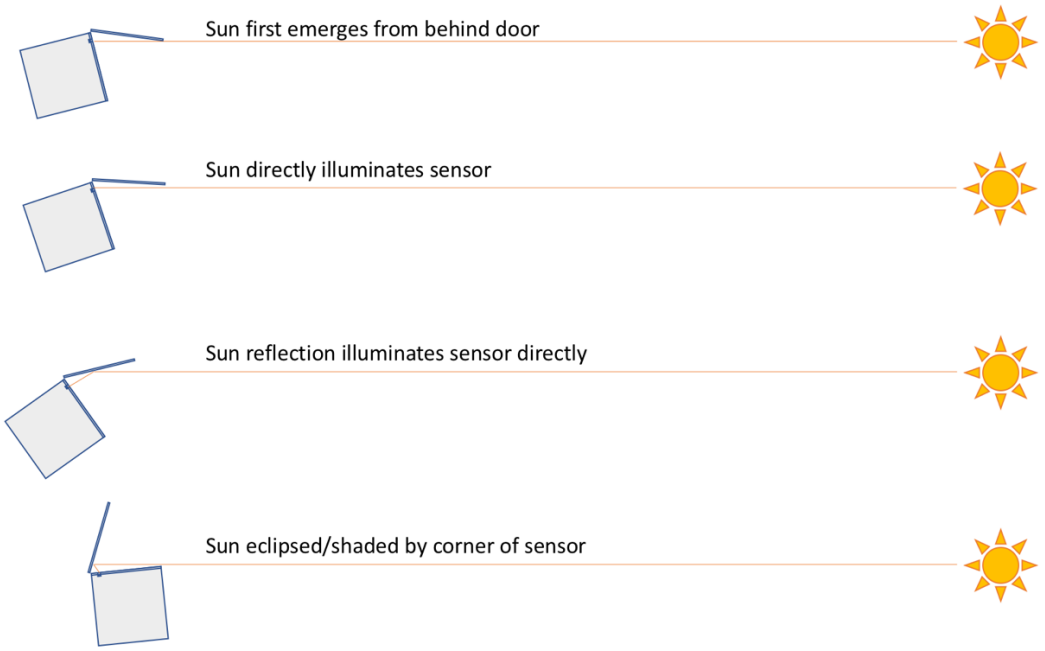

Figure 12. Scanning the 45-degree sensor vertically shows some configurations that will be encountered.

Table 4. Test 3: 45-degree, vertical

Angle (deg)	Sun (V)	Sun (hex)	Comment
10	0.031	026	
15	0.015	013	
20	0.015	012	
25	0.028	023	
30	0.108	086	
35	0.196	0F3	
40	0.237	127	
45	0.214	10A	
47.5	0.134	0A6	Mirror reflection crosses sensor
50	0.071	057	
55	0.039	031	
60	0.017	015	
64	0.011	00E	Direct sun, no mirror
65	0.011	00E	"
70	0.019	017	"
75	0.059	049	"

Angle (deg)	Sun (V)	Sun (hex)	Comment
77	0.075	05D	Direct sun, no mirror
80	0.004	005	Door shadow crosses sensor
85	0.004	005	
60	0.017	015	
50	0.068	055	
47.5	0.108	087	
46	0.208	101	
44	0.221	112	
42	0.235	123	
40	0.240	129	
38	0.230	11D	
36	0.203	0FC	
34	0.174	0D8	
32	0.142	0B1	
30	0.113	08C	
28	0.071	058	

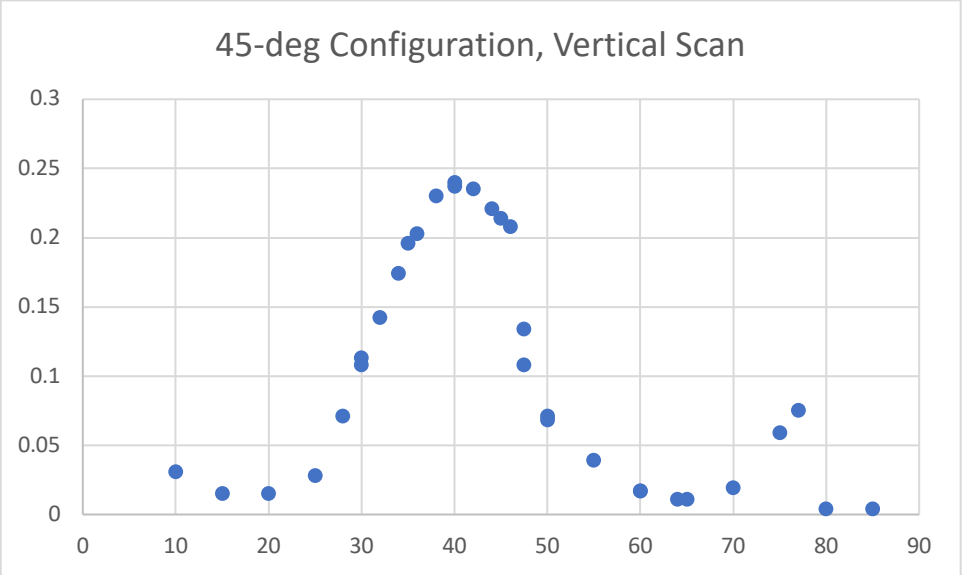

Figure 13. For this case, the door is only open 90°-22.5°= 67.5°, which corresponds approximately to the non-zero measurements in the graph above. Note that the main signal is still about 18° degrees FWHM, but that the glints seen roughly ±40° off-axis are cut off by doors or shading.

2.5 LIMB Configuration, vertical direction 2019/12/20

The occurrence of shadows, reflections, and direct sun will be qualitatively similar to the limb configuration (Figure 12), with some expected differences in the angular values, because the door is opened to 54° =(90°+18°)/2, rather than the 67.5°=(90°+45°)/2 position. However, due to an error during testing an opening of 72° was tested, corresponding to a limb angle of 81°. The position of the pickoff as tested therefore allows a slightly larger acceptance angle than the 45° configuration; however, the angular dependences among tested configurations remains valid.

Table 5. Test 4: Limb configuration, vertical

Angle (deg)	Sun (V)	Sun (hex)	Comment
10	0.236	125	Initially maximized signal
-15	0.004	005	Reflected shadow of front face crosses detector
-10	0.013	00E	
-5	0.020	018	
0	0.083	067	
2	0.121	-	
4	0.157	0C3	
6	0.196	0F3	
8	0.226	119	
10	0.236	125	
12	0.222	114	
14	0.192	0EE	
16	0.161	0C8	

Angle (deg)	Sun (V)	Sun (hex)	Comment
18	0.124	09A	
20	0.085	069	
24.5	0.030	025	
30	0.019	018	
35	0.017	015	Seeing direct sun
40	0.029	024	
45	0.066	052	
50	0.068	054	
55	0.035	02D	
60	0.017	015	Door shadow near sensor
63	0.006	007	Door shadow crosses sensor
65	0.004	005	Sensor shadowed
70	0.004	005	Sensor shadowed

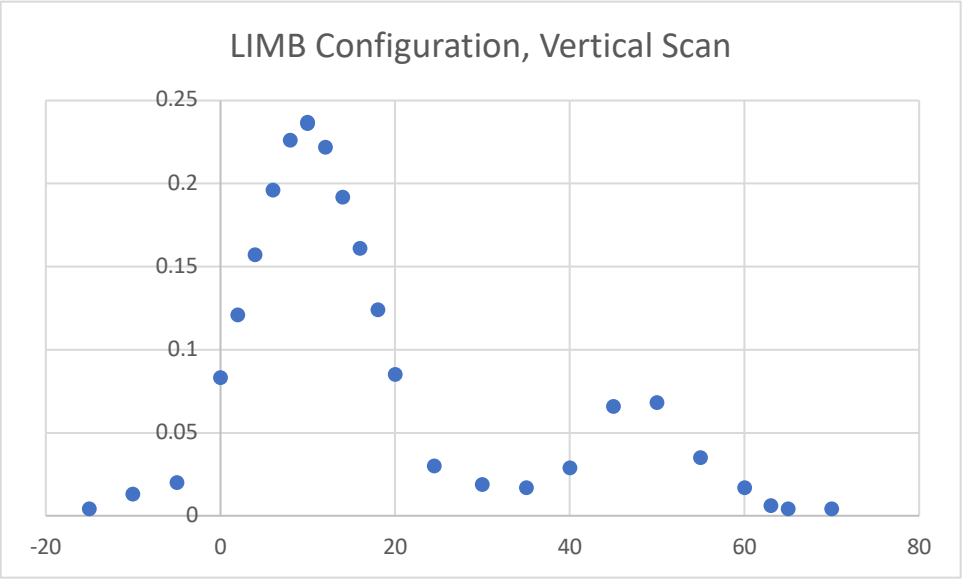

Figure 14. For this case, the door is open wider to 90°-18°=72° seen in the non-zero values again. Note that the main signal is still about 16° degrees FWHM. The left off-axis glint of the previous figure is cut off by the shading of the door, but the other secondary glint is present.

2.6 LIMB Configuration, horizontal direction 2019/12/20

The cross-track behavior of all configurations is expected to be similar, due to the presence of dog-ear shades in all Tri-TIP sensors. Two cases were checked: first a cross-track sweep with the sun signal maximized in-track, followed by a second cross-track sweep with the sun 7.5° off-peak in-track. Note that since the sun sensor is much closer to one dog-ear than to the other, the sun angle is expected to be highly asymmetrical in the cross-track direction.

Table 6. Test 5: Limb configuration, horizontal

Angle (hrs)	Angle (deg)	Sun (V)	Comment
3:35	53.75	0.233	Initial. Maximized signal
0:45	11.25	0.004	
1:00	15.00	0.005	
1:15	18.75	0.052	
1:30	22.50	0.068	
1:45	26.25	0.048	
2:00	30.00	0.03	
2:15	33.75	0.031	
2:30	37.50	0.078	
2:45	41.25	0.138	
3:00	45.00	0.192	
3:15	48.75	0.236	
3:30	52.50	0.239	
3:45	56.25	0.228	
3:55	58.75	0.222	
3:35	53.75	0.233	
4:00	60.00	0.215	
4:05	61.25	0.045	Shadow crosses sensor
4:15	63.75	0.003	Past shadowed edge

Angle (hrs)	Angle (deg)	Sun (V)	Comment
3:35	53.75	0.084	Sun intentionally not maximized
4:15	63.75	0.004	Past shadowed edge
4:00	60.00	0.085	
3:45	56.25	0.084	
3:30	52.50	0.083	
3:00	45.00	0.077	
2:30	37.50	0.053	
2:00	30.00	0.023	

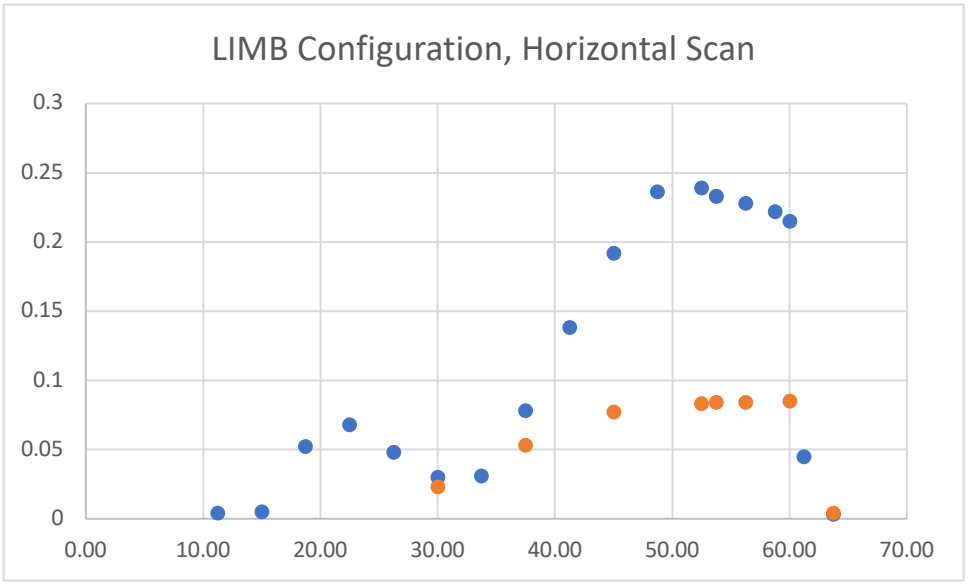

Figure 15. For this case the door in configured for limb viewing, but the scan is performed in the cross-track (horizontal) direction. As expected, the sun signature is highly asymmetric. The cross-track width appears wider with FWHM of >19°, consistent with expectation (blue). When the Sun does not pass across the center of the field-of-view the signal is both low and flatter (red). Note that the point at 63.75° is at the background level for both the blue and over-plotted red point.

2.7 Outdoor Test Set-up and Procedure

2.7.1 Equipment required:

- ESD statics pad, wrist strap, and cart
- Tri-TIP EM unit, a black Kapton EM aperture mask, EM test adapter board, HV red warning light, electrical harnesses, and laptop computer
- Test adapter EGSE software
- Dual low voltage power supply (+/-/GND)
- Four multimeters to monitor voltages and currents

Figure 16. The rooftop set-up for testing EM sun sensor reponse to direct sunlight.

2.7.2 Test Procedure

The outdoor sun sensor test should be performed on the EM unit on a clear, sunny day.

1. Make sure the EM aperture is covered by the opaque, black Kapton tape cover. Tape the mirror door open into NADIR configuration. Tape a small, clean stick on the outside of the sensor parallel to the optical path.
2. Perform electrical initialization as per the set-up procedure, followed by a functional test to ensure all connections have been made

properly and the EM unit is functional.

3. Using gloved hands and all electrostatic precautions, point the sun sensor directly at the Sun by minimizing the shadow of the affixed stick. Maximize the sun sensor signal and record results.

2.8 Signal Measurement for Direct Sun 2019/12/26

All the tests to this point have been performed using a laboratory synthetic sun. The maximum brightness of the sun-lamp is about 1/3 that of the sun, and we used the lamp at about 50% brightness. In addition, the peak sensitivity of the photodiode occurs at 0.94 µm according to the data sheet [OSI Optoelectronics, 2015], whereas the Sun peaks in the visible portion of the spectrum. Consequently, the apparatus was taken to the roof of Building 209 to observe the sun sensor response to direct sunlight. Due to both atmospheric attenuation and light cirrus clouds on the day of measurement (Figure 16), we expect the response of sensors to sunlight on orbit to be greater than measured in the ground test.

Table 7. Test 6: Direct Sun Response for the Sun Sensor

Maximum (V)	Maximum (hex)
1.865	0x0912

The value of signal near the maximum solar signal was 1.5-1.7 V, with a peak value somewhat higher. This value is about 7X the maximum NADIR signal observed in the laboratory, which is consistent with expectations. The reflection off of the pick-off mirror in 45F, 45R, and LIMB is expected to result in a somewhat lower peak sun signal than this nadir configuration.

3. SUMMARY

The field-of-view of the sun sensor aboard Tri-TIP was observed to be generally consistent with the mechanical design. Shadowing and reflections around the sun sensor add complexity to the response to solar illumination within the field-of-view. Laboratory measurements showed that

- The in-track (vertical) field-of-view is 16-18° FWHM. Generally, this full field-of-view is accessible to the sun sensor.
- The cross-track (horizontal) field-of-view is only 19° wide and very asymmetrical at FWHM due to shadowing by the dog-ears, but is consistent with a wider cross-track field-of-view.
- Secondary vertical responses may arise from reflections from the Tri-TIP walls at the sun-sensor viewing port, centered about ±40° on either side of the center and about 30% the peak magnitude.
- The Sun signal from rooftop measurements was 1.8V or 0x912 in raw A/D values.

Recommendations for follow-on sensors that may be implemented in future versions of Tri-TIP and other sensors are:

- The threshold for the Sun should be raised above the levels expected for the secondary reflections (30% of 0x912 peak = 0x02B9). This would be higher than the default level of 0x126, and provide a wider safety margin than the FWHM values.

- The threshold should be set above the value observed for sunlit clouds, to ensure that timeouts are not set on the dayside Earth. This can be determined on orbit during early orbit testing. (This will probably be below the threshold to eliminate the secondary peaks.)
- Future instruments might minimize the reflections near the photodiode generating the secondary peaks if the sidewalls of the sun sensor viewports are threaded holes or countersunk knife edges.

REFERENCES

S. A. Budzien, A. W. Stephan, K. F. Dymond, C. M. Brown, P. J. Marquis, and A. C. Nicholas 2018, "Three-Channel Airglow Photometer Data Analysis Methodology", NRL Memorandum Report NRL/MR/7634--18-9802, (Naval Research Laboratory, Washington, DC).

K. F. Dymond, A. C. Nicholas, S. A. Budzien, A. W. Stephan, P. Marquis, C. M. Brown, T. Finne, and K. D. Wolfran 2017, "Low-latitude ionospheric research using the CIRCE Mission: instrumentation overview," *Proc. SPIE 10397, UV, X-Ray, and Gamma-Ray Space Instrumentation for Astronomy XX*, 1039719 (O. H. Siegmund, ed., Bellingham, WA), doi:10.1117/12.2275336.

K. F. Dymond, S. A. Budzien, and M. A. Hei 2017, "Ionospheric-thermospheric UV tomography: 1. Image space reconstruction algorithms", *Radio Science*, **52**, 338-356, doi :10.1002/2015RS005869.

Andrew C. Nicholas, Gemma D. R. Attrill, Kenneth F. Dymond, Scott A. Budzien, Andrew W. Stephan, Bruce A. Fritz, Graham J. Routledge, Junayd A. Miah, Charles M. Brown, Peter J. Marquis, Ted T. Finne, Cathryn N. Mitchell, Robert J. Watson, Dhiren O. Kataria, and James Williams 2019, "Coordinated Ionospheric Reconstruction CubeSat Experiment (CIRCE) mission overview," *Proc. SPIE 11131, CubeSats and SmallSats for Remote Sensing III*, 111310E (Thomas S. Pagano, Charles D. Norton, Sachidananda R. Babu, eds., Bellingham, WA), doi:10.1117/12.2528767.

OSI Optoelectronics, Inc. 2015, "Photovoltaic Series: Planar Diffused Silicon Photodiodes", *Optoelectronic Components Catalog*, http://www.osioptoelectronics.com/application-notes/osi_parts_catalog.pdf